MAP kinase signaling induces nuclear reorganization in budding yeast

Elisa M. Stone*†, Patrick Heun‡, Thierry Laroche‡, Lorraine Pillus* and Susan M. Gasser‡

Background: During the mating pheromone response in budding yeast, activation of a mitogen-activated protein kinase (MAP kinase) cascade results in well-characterized changes in cytoskeletal organization and gene expression. Spatial reorganization of genes within the nucleus has been documented during cell-type differentiation in mammalian cells, but no information was previously available on the morphology of the yeast nucleus during the major transcriptional reprogramming that accompanies zygote formation.

Results: We find that in response to mating pheromone, budding yeast nuclei assume an unusual dumbbell shape, reflecting a spatial separation of chromosomal and nucleolar domains. Within the chromosomal domain, telomeric foci persist and maintain their associated complement of Sir proteins. The nucleolus, on the other hand, assumes a novel cup-shaped morphology and a position distal to the mating projection tip. Although microtubules are required for this orientation with respect to the projection tip, neither microtubules nor actin polymerization are necessary for the observed changes in nuclear shape. We find that activation of the pheromone-response MAP kinase pathway by ectopic expression of *STE4* or *STE11* leads to identical nuclear and nucleolar reorganization in the absence of pheromone. Mutation of downstream effector MAP kinases Fus3p and Kss1p, or of the transcriptional regulator Ste12p, blocks nuclear shape changes, whereas overexpression of Ste12p promotes

Conclusions: Nuclear remodeling occurs when the MAP kinase cascade is activated by yeast pheromone, but it is independent of the cytoskeletal reorganization regulated by the same signaling pathway. Activation of the Ste12p transcription factor is necessary, and may be sufficient, for the changes in nuclear structure that coincide with developmentally significant changes in gene expression.

Addresses: *Department of Biology, University of California at San Diego, 9500 Gilman Drive, La Jolla, California 92093-0347, USA. ‡Swiss Institute for Experimental Cancer Research (ISREC), Chemin des Boveresses 155, CH-1066 Epalinges/Lausanne, Switzerland.

Present address: †Science and Health Education Partnership, University of California, San Francisco, 100 Medical Center Way, San Francisco, California 94143-0905, USA.

Correspondence: Lorraine Pillus or Susan M. Gasser
E-mail: lpillus@biomail.ucsd.edu; sgasser@eliot.unil.ch

Received: **7 December 1999**
Revised: **31 January 2000**
Accepted: **11 February 2000**

Published: **20 March 2000**

Current Biology 2000, 10:373–382

0960-9822/00/$ – see front matter

Background

The eukaryotic nucleus is organized into various subcompartments, each optimized for the execution of particular functions (for review, see [1–3]). Its most obvious subcompartment is the nucleolus, which supports the transcription and processing of rRNA for ribosome biogenesis. In addition, chromosomes themselves have been shown to occupy discrete subnuclear territories [4], although interchromosomal contacts exist. For example, centromeric heterochromatin in *Drosophila* clusters to form the chromocenter, which associates preferentially with the nuclear envelope [5]. Similarly, in the budding yeast *Saccharomyces cerevisiae*, the silent chromatin of subtelomeric genes and the *HM* loci are found in foci near the periphery of the nucleus [6,7].

In fission yeast (*Schizosaccharomyces pombe*), the subnuclear positions of centromeres and telomeres change during vegetative growth and in the early stages of meiosis. Telomeres in premeiotic zygotic cells, for example, cluster near the spindle pole body (SPB, the yeast centrosome) at the periphery of the elongated 'horse-tail' nucleus that is formed by nuclear fusion. This telomeric cluster then leads the chromosomes in a rapid oscillating movement that appears to facilitate the meiotic pairing of homologs [8,9]. A functional link between this telomeric positioning, transcriptional silencing, and meiotic recombination in *S. pombe* is suggested by their coordinated loss in strains lacking the telomere-binding protein Taz1p [10,11]. Similarly, the absence of the telomere-binding proteins yKu70 or yKu80 in budding yeast leads to a loss of telomere clustering and subtelomeric silencing [12,13], and an enhanced level of mitotic recombination between telomeric and internal chromosomal regions [14].

Several studies have examined the spatial positioning of *S. cerevisiae* centromeres and telomeres in meiotic and

mitotic cells [6,15–20]. In G1 phase, centromeres are found in the vicinity of the SPB, while telomeres are perinuclear, and centromeres lead chromosomal movement into the bud during nuclear division. In the pre-pachytene meiotic nucleus, telomeres appear to aggregate transiently in a cluster before they become dispersed throughout the nucleus [18–20]. Although both telomeres and rDNA repeats are sites of chromatin-mediated transcriptional silencing, these domains do not colocalize. Rather, the nucleolus forms a crescent-shaped cap over one side of the genomic DNA, abutting the nuclear envelope (see for example [21]). In contrast to the situation in multicellular eukaryotes, in which the nucleolus disassembles as chromosomes condense [22], the yeast nucleolus persists throughout mitosis and partitions between the two daughter cells. In yeast, nucleolar morphology depends on both the presence of RNA polymerase I and the copy number of the tandem rDNA repeats [23,24]. In aging cells, the excision of rDNA circles by recombination results in fragmentation and repositioning of the nucleolus within the nucleus [25].

During the response to mating pheromone, signaling involving mitogen-activated kinase (MAP kinase) triggers major changes in gene expression and cellular architecture that are necessary for the mating process (reviewed in [26,27]). To date, however, no one has reported whether there are changes in nuclear organization as haploid cells prepare for conjugation. Here we follow the morphology of the yeast nucleus during the response to pheromone, and document a major restructuring of both the nucleus and the nucleolus in response to the MAP kinase cascade. These events are independent of microtubule integrity and actin polymerization, and can be elicited by activation of Ste11p, a MAP kinase/ERK kinase kinase (MEKK), in the absence of pheromone. Intriguingly, activation of the transcriptional regulator Ste12p appears to be sufficient for at least part of the observed nuclear reorganization, even when elements of the upstream signaling cascade are inactive.

Results

Nuclear and nucleolar reorganization occurs during the mating response

Using fluorescence microscopy to visualize chromosomal DNA, the nucleolus and the nuclear envelope, we examined whether nuclear restructuring occurs as yeast cells respond to the mating pheromone, α factor. Our initial observations make use of a *MAT***a** strain carrying green fluorescent protein (GFP)-tagged nuclear pore protein (GFP–Nup49p), which allows us to monitor nuclear dynamics in living cells by phase-contrast and fluorescence microscopy, following addition of α factor. In unbudded G1-phase cells, the nucleus is round and measures roughly 2 μm in diameter (Figure 1a). After exposure to pheromone, the nucleus nearly doubles in size, adopting a dumbbell shape (Figure 1b). This coincides with distortion of the cell into the characteristic pear-shaped pheromone-stimulated yeast cell ('shmoo'). Confocal sectioning of these cells confirms that there is an increase in nuclear volume and not a 'flattening' of the nuclear sphere (data not shown). To determine whether this nuclear reorganization occurs naturally during mating, a *MAT***a** strain

Figure 1

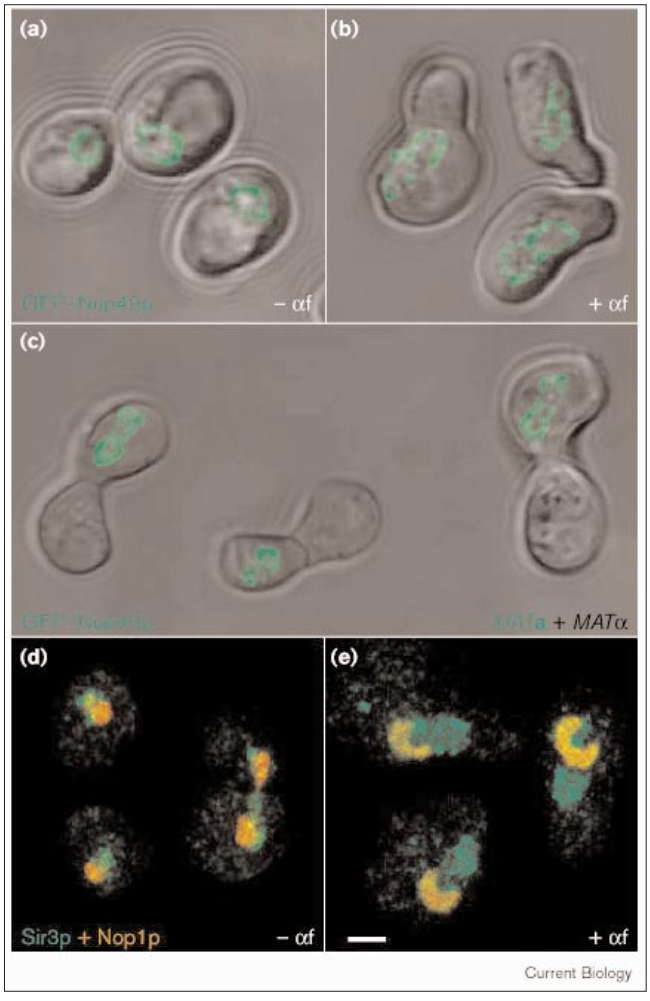

Pheromone treatment induces nuclear reorganization in budding yeast cells. **(a,b)** GA-1109 cells growing asynchronously or treated with α factor (αf) for 2.5 h were examined alive by direct fluorescence of the nuclear pore protein construct GFP–Nup49p. The staining of the nuclear envelope (green) was merged with a phase-contrast image of the cells (gray). **(c)** The *MAT***a** strain GA-1096 expressing GFP–Nup49p was mated with the *MAT*α strain W303-1b for 4 h. Zygotes in the process of formation were examined by phase-contrast microscopy, and the nuclear envelope was detected with direct GFP fluorescence in only one of each mating pair. **(d,e)** *MAT***a** cells (LPY2686) (d) growing asynchronously or (e) treated with α factor were processed for immunofluorescence. Cells were stained with affinity-purified antibodies against Sir3p (green) to identify telomeres and against Nop1p (red) to identify the nucleolus. Ethidium bromide stains both nuclear domains (data not shown). Note that the cell on the right in (d) is undergoing mitosis, and that the nucleolus segregates normally as described in [38]. Images were collected on a Zeiss LSM 410 confocal microscope. The scale bar represents 2 μm.

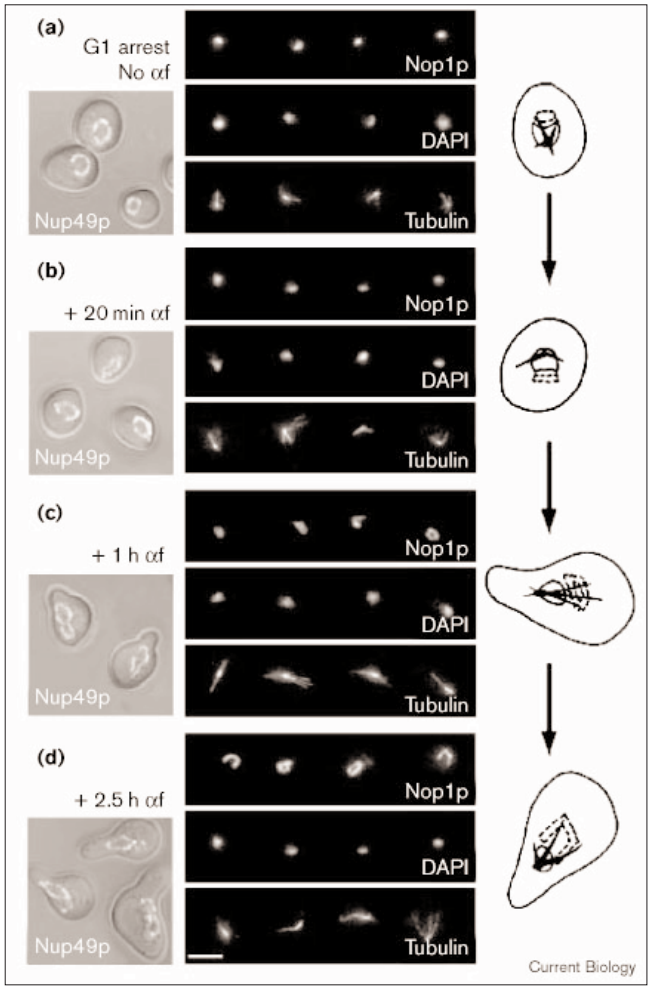

Figure 2

The nucleolus undergoes structural reorganization during the pheromone response. A synchronous pheromone response was achieved by arresting strains 1608-21C or GA-1163 by G1 cyclin depletion followed by exposure to α factor (αf). The strains used lack all three *CLN* G1 cyclin genes, but are kept alive by expressing *CLN3* under the control of the inducible *GAL1,10* promoter [56]. Consequently, this strain arrests at START when switched from galactose to glucose medium. **(a)** Cells arrested in G1 after 2.5 h in glucose, were treated with 1 μg/ml α factor, and were harvested at **(b)** 20 min, **(c)** 1 h and **(d)** 2.5 h. Phase-contrast microscopy and direct GFP–Nup49p nuclear envelope fluorescence were performed in parallel on live cells (left panels). The center panels show indirect immunofluorescence on fixed cells triple-stained with anti-Nop1p, DAPI, and anti-tubulin, as labeled. Nop1p and DAPI signals do not overlap. Four cells are shown for each time point, and a representative diagram of one of these is given on the right. In the diagrams, a typical spherical nucleolus, represented by a dashed line in (a), elongates into a bar shape (b), and progresses into a diffuse structure (c) that becomes a distinct cup shape (d). For quantitation see Table 1. These changes in nucleolar morphology were also seen in wild-type haploid cells (data not shown). GFP–Nup49p images were collected on a Zeiss LSM 410 confocal, the others on a Zeiss fluorescence microscope. The scale bar represents 2 μm.

expressing the GFP–Nup49 nuclear envelope marker was mixed with an untagged *MAT*α strain to initiate mating. After 4 hours at room temperature, the mixture was examined by fluorescence microscopy. We noted that before cells of opposite mating type fused at their projection tips, the majority of GFP-tagged nuclei assumed a pronounced dumbbell shape (Figure 1c). Thus, changes in nuclear size and shape occur before nuclear fusion during the mating process, and in cells exposed to pheromone *in vitro*.

To determine whether the two halves of the distorted nucleus represent distinct compartments, we stained pheromone-treated *MAT***a** cells for Nop1p and Sir3p, which are markers for nucleolar and subtelomeric chromatin, respectively. Rather than finding the nucleolus as a cap over the mass of genomic DNA, we see striking separation of the two staining patterns (compare Figure 1d and 1e). The nucleolus becomes enlarged, and assumes a cup-shaped morphology, occupying one side of the bilobed nucleus. The other lobe contains the rest of the genomic DNA, including the telomeres, as represented by Sir3p staining. General dyes for DNA, such as 4′6-diamidino-2-phenylindole (DAPI), colocalize with Sir3p in the non-nucleolar lobe (data not shown).

During mating, yeast cells that are exposed to pheromone complete their current cell cycle and accumulate in late G1, where they arrest at START and initiate characteristic changes in cytoskeletal organization and gene transcription (reviewed in [27]). To study the kinetics of the observed nuclear distortion, we synchronized cells in G1, by depleting for G1 cyclins, before the addition of α factor. Pheromone-treated and untreated G1-phase cells were compared at 20 minutes, 1 hour and 2.5 hours by staining with markers for the nucleolus (anti-Nop1p), microtubules (anti-tubulin) and genomic DNA (DAPI). In parallel, cellular morphology and nuclear shape were monitored in living cells, using a similarly synchronized population of cells expressing the GFP–Nup49p marker.

The cells and nuclei of the culture arrested in G1 are round or slightly oval before exposure to α factor (Figure 2a, Table 1), with a crescent-shaped nucleolus positioned at one side of the nucleus. After 20 minutes of exposure to α factor, the first signs of projection tip formation occur, coinciding with a distortion of nuclear shape. A fraction of cells also exhibits changes in nucleolar morphology, visible as a slightly elongated or bar-shaped nucleolus (Figure 2b, Table 1). By 1 hour, as the projection tip of the shmoo becomes clearly visible, a majority of cells have dumbbell-shaped nuclei. By this time, the nucleolus becomes separated from the mass of DAPI-stained chromatin and assumes a shape reminiscent of a diffuse cup or lasso (Figure 2c, Table 1).

By 2.5 hours, pronounced projection tips and elongated, dumbbell-shaped nuclei are seen in almost all cells, and nearly 80% of the nucleoli have cup or lasso shapes (Figure 2d, Table 1). We interpret the lasso morphology to

Table 1

Nucleolar morphology changes progressively during exposure to mating pheromone.

	Spherical/ crescent (%)	Bar shaped (%)	Diffuse cup/ lasso (%)	Structured cup/lasso (%)
G1 phase, no αf*	94	3	0	3
20 min αf†	76	18	6	0
1 h αf‡	42	8	33	17
2.5 h αf§	15	7	24	54
Mock, + 2.5 h αf#	6	8	30	56
Noc, + 2.5 h αf¶	7	7	38	48

The experiments shown in Figure 2a–d and in Figure 4b are quantified here. Sample size, $^{*}n = 191$, $^{\dagger}n = 131$, $^{\ddagger}n = 114$, $^{\S}n = 107$, $^{\#}n = 228$ and $^{\P}n = 228$. The addition of α factor is indicated by αf. Analysis using a standard χ^2 test revealed that the nucleolar shapes change during the α factor time course, with statistical significance to $p < 0.001$. The bottom two rows reflect the untreated (mock) and nocodazole-treated (Noc) samples shown in Figure 4b. Although the distribution of diffuse versus structured cup or lasso shapes is slightly shifted, the sum of diffuse and structured cup or lassos is identical in the two samples.

be a cross-section of the cup-shaped domain, and thus indicative of the same structure. Simultaneous staining with anti-tubulin antibodies revealed that microtubules extend from both faces of the SPB at the edge of the nucleus closest to the projection tip (data not shown, and Figure 2c, tubulin), consistent with previous observations [28–32].

Characterization of telomeric and nucleolar localization within nuclei of pheromone-responding cells

Prompted by observations that the telomere-associated silencing factor Sir3p is phosphorylated in response to MAP kinase activation in budding yeast [33], and that telomeres migrate to a single site in the zygotic nucleus of fission yeast [8,9], we asked whether telomere clustering changes in the presence of pheromone. The enrichment of the three yeast silencing factors Sir2p, Sir3p and Sir4p at telomeric foci correlates with the maintenance of a repressive chromatin structure in subtelomeric DNA [6,21], enabling us to monitor telomere positioning and the integrity of telomere-associated heterochromatin by fluorescent *in situ* hybridization (FISH) and indirect immunofluorescence, respectively. In both vegetatively growing (– αf) and pheromone-treated (+ αf) cells, we observed a pattern of seven to nine telomeric foci per nucleus, revealed by the subtelomeric Y′ probe (Figure 3a,b) and by anti-Sir3p staining (Figure 3c,d). Similar results were obtained for the localization of the telomere-bound factor Rap1p (Repressor activator protein 1), and Sir4p (data not shown). These results suggest that Sir proteins remain associated with the telomere and that telomeres maintain their pattern of clustering in the presence of α factor. The elongation of the nucleolar domain in response to pheromone treatment is readily visible in these images, because ethidium bromide, unlike DAPI, efficiently stains nucleolar RNA as well as the genomic DNA.

Figure 3

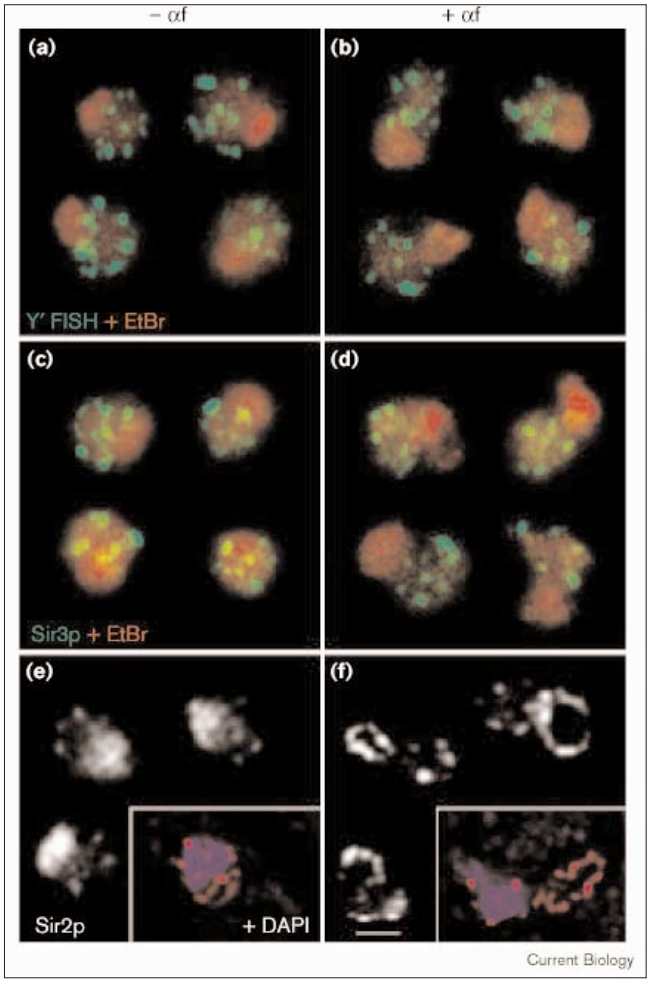

Telomeres remain clustered, and the nucleolus forms a spatially distinct domain within the nucleus of pheromone-responding cells. **(a,c,e)** The yeast strain LPY2686 grown asynchronously without α factor (– αf); **(b,d,f)** the same strain treated with α factor (+ αf). All cells were subsequently processed for immunofluorescence or FISH. (a,b) FISH was performed with the subtelomeric Y′ repeat (green) and DNA was counterstained with ethidium bromide (EtBr, red). (c,d) Cells were labeled with affinity-purified anti-Sir3p (green) and counterstained as described above. No major rearrangements are observed for telomeric DNA or Sir3p distribution in the presence or absence of α factor. (e,f) Cells were stained with affinity-purified anti-Sir2p to identify telomeres and the nucleolus. The insets show Sir2p staining (red) combined with DAPI (blue) to identify chromosomal DNA. DAPI does not stain the nucleolus. In pheromone-treated cells, Sir2p staining becomes bead-like in an extended nucleolus that is separated from the DAPI signal. Images were collected on a Nikon epifluorescence microscope. The scale bar represents 2 μm.

The silencing protein Sir2p is essential for the chromatin-mediated repression of RNA polymerase II-transcribed reporter genes in subtelomeric regions and within the

rDNA [34–37]. Sir2p consistently localizes to both sites in vegetatively growing cells [21] (Figure 3e). Although the Sir2p staining at telomeres in pheromone-treated cells is quite similar to that of a vegetatively growing culture (compare Figure 3e and 3f), we observed a more pronounced 'beaded' appearance for nucleolar Sir2p in the treated cells (Figure 3f). Moreover, the combination of Sir2p immunofluorescence with DAPI, which detects only the genomic DNA, highlights the spatial separation of the nucleolus from the chromosomal DNA (Figure 3f, inset). Sir2p is restricted to a subset of the extended nucleolar structure detected by Nop1p (data not shown), consistent with its proposed interaction with the rDNA repeats [21,36].

Nuclear and nucleolar restructuring is independent of microtubules

Because the SPB in vegetatively growing cells is positioned opposite the nucleolus [38], and because the single SPB is directed towards the projection tip of pheromone-responding cells [28–32], it seemed likely that the nucleolar domain of the dumbbell nucleus was oriented away from the projection tip during the pheromone response. Simultaneous detection of telomeres (anti-Sir3p), and the actin-containing projection tip (anti-actin) showed that the Sir3p-stained domain is proximal to the actin-stained projection tip in 89% of shmoos (Figure 4a, + αf). In contrast, nuclear orientation in growing cells appears random with respect to the bud site (Figure 4a, – αf), which, like the projection tip, represents the site of preferential plasma membrane and cell-wall growth.

To investigate whether nucleolar reorganization requires the microtubule network, we treated cells with the microtubule-depolymerizing agent nocodazole and again looked for changes in nucleolar morphology following the addition of α factor. Cells were first synchronized at START by depletion of G1 cyclin, and were then exposed either to nocodazole or to solvent alone for 30 minutes. Controls confirmed the loss of microtubules in nocodazole-treated cells (data not shown). Cells were then exposed to α factor for 2.5 hours, fixed, and stained for Nop1p, actin and Sir proteins. We observed very similar pheromone-induced

Figure 4

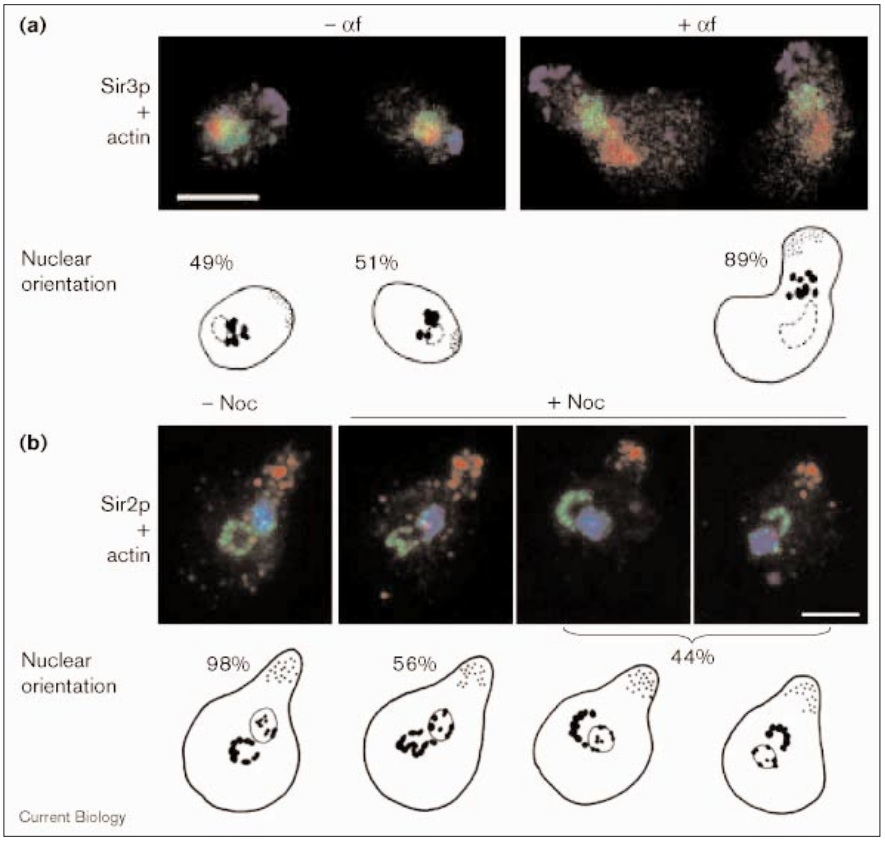

The nucleus orients with specific positioning relative to the polarized mating projection tip of pheromone-responding cells. **(a)** Asynchronously growing LPY2686 cells or cells treated with α factor (αf) were stained with anti-Sir3p (green) and anti-actin (blue) antibodies. Sir3p identifies telomeric foci and actin identifies the bud site in mitotically growing cells or the mating projection tip in cells responding to pheromone. Ethidium bromide (red) preferentially stains the nucleolus. In asynchronous cells, the nucleolus was distal to the bud site in 49% of the cells, whereas in 51% of the cells there was no preferential organization (sample size, $n = 41$). With pheromone, the telomeric domain oriented specifically toward the projection tip in 89% of the cells ($n = 65$). Analysis using a standard χ^2 test demonstrated statistical significance to $p > 0.001$. The scale bar represents 5 μm. Images were collected on a Zeiss LSM 410 confocal microscope. Sketches representing immunofluorescence images are below each stained cell. **(b)** Strain 1608-21C was arrested at START as described in Figure 2, and cells were either untreated, or treated with nocodazole to disrupt microtubules, followed by exposure to α factor. To monitor subcellular structures, cells were stained with anti-Sir2p (green) to identify telomeres and the nucleolus, with anti-actin (red) to identify the mating projection tip, and with DAPI (blue) to identify the chromosomal domain. In 98% of the G1-arrested cells not treated with nocodazole, the nucleolus is distal to the projection tip ($n = 107$). In nocodazole ($n = 99$), this value drops to 56%. The remaining 44% contained nuclei in which nucleolar and chromosomal domains were equidistant from, or pointing towards, the projection tip. Standard χ^2 analysis revealed statistical significance to $p > 0.001$. Images were collected on a Leica DMRXA microscope. The scale bar represents 5 μm.

nuclear and nucleolar changes in the presence or absence of nocodazole (Table 1, Figure 4b), ruling out a major role for microtubules in these events.

To evaluate the role of microtubules in the rotational positioning of the nucleus, we asked whether the preferential orientation of the nucleolus away from the shmoo tip is altered by incubation in nocodazole. Cells treated as described above were scored simultaneously for their staining patterns for DAPI, Sir2p and actin. The chromosomal domain was positioned closest to the projection tip in 98% of the pheromone-treated cells (similar to the value obtained after Sir3p staining, see Figure 4). In the presence of both nocodazole and pheromone, this orientation was observed in only 56% of the cells (Figure 4b, + Noc). In the remaining population, nucleoli assumed more random positions with respect to the actin staining (Figure 4b, + Noc). This confirms and extends the observations of Read *et al.* [32], who noted that the DAPI-stained portion of the nucleus shifts away from the projection tip, toward the anterior portion of the shmoo, in actin and tubulin mutants. In conclusion, we find that the rotational orientation of the nucleus in cells responding to pheromone is microtubule-dependent, but that nuclear and nucleolar restructuring are not.

Figure 5

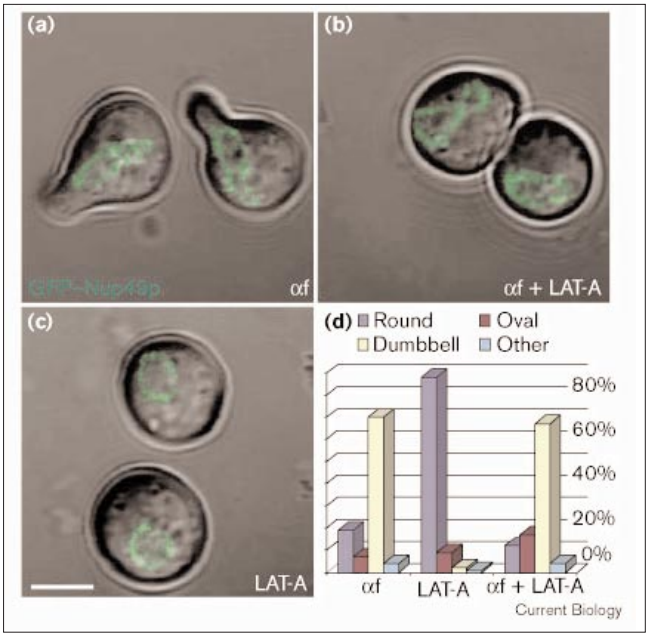

Pheromone-induced changes in cellular, but not nuclear, morphology require actin polymerization. The strain GA-1163 expressing GFP–Nup49p for detection of the nuclear envelope was arrested by G1 cyclin depletion (see Figure 2). After G1 arrest, cells were incubated **(a)** in the absence or **(b,c)** in the presence of 400 μM latrunculin-A (LAT-A) to disrupt actin polymerization. Incubation was continued (a,b) in the presence or (c) in the absence of 1 μg/ml α factor for 90 min. Nuclear shape was monitored by direct GFP fluorescence (green), which was superimposed on the phase-contrast image of the cells (grey). **(d)** The distribution of the nuclei into round, oval, dumbbell or distorted (other) shapes was scored for 100 nuclei under each condition and is shown as a graph. Images were collected on a Zeiss LSM 410 confocal microscope. The scale bar represents 4 μm.

Pheromone-induced nuclear reorganization does not require polymerized actin

In view of the important role of the actin cytoskeleton in shmoo formation [32,39], we next tested whether the pheromone-induced nuclear restructuring occurs when actin assembly is disrupted. This is achieved by the addition of the drug latrunculin-A (LAT-A). Because LAT-A can also arrest nuclear division in cells progressing from the G2 phase to the M phase, the culture was again synchronized at START by depletion of G1 cyclin, and then incubated with LAT-A before addition of α factor. As previously reported, LAT-A treatment prevents formation of the mating projection tip (Figure 5a,b, and [39]). Nevertheless we observed the characteristic dumbbell nuclear shape in 85% of the cells exposed to pheromone (Figure 5b,d). In controls, an equivalent incubation of G1-phase cells with LAT-A alone had no effect on the spherical shape of the nucleus (Figure 5c). This indicates that the pheromone-induced nuclear reorganization does not require actin polymerization, and can occur in the absence of cytoplasmic rearrangements.

Activation of the MAP kinase signaling pathway elicits nuclear reorganization

Pheromone exposure initiates signal transduction through a well-characterized MAP kinase cascade to activate genes required for the mating response. To determine whether this cascade or another pheromone-activated response elicits nuclear reorganization, we stimulated the MAP kinase pathway in the absence of pheromone, using a galactose-inducible *STE4* gene. *STE4* encodes the β subunit of a trimeric G protein, expression of which activates downstream elements of the MAP kinase cascade (Figure 6a). When *GAL–STE4* was repressed in the presence of glucose, nuclear morphology appeared normal and all the cells in the population had spherical or crescent-shaped nucleoli (Figure 6b). In contrast, after a 6 hour induction of *GAL–STE4*, nucleolar morphology became extended as the nucleolus separates from the genomic DNA (Figure 6c). The distinctive nucleolar cup shape shown in Figure 2 was found in ~81% of the cells. Anti-tubulin staining revealed SPBs and associated microtubules typical of either vegetatively growing cells (Figure 6b) or shmoos (Figure 6c). Moreover, among the *GAL–STE4*-induced cells with reorganized nucleoli, over 90% of the nuclei were oriented with the chromosomal domain towards the projection tip (data not shown).

As *STE4* functions upstream of the MAP kinase cascade and may possibly affect other pathways, we also used a galactose-inducible, constitutively active form of the MEKK Ste11p

(*STE11–Asp3*; F. van Drogen and M. Peter, personal communication) to confirm that MAP kinase activation alone is sufficient to elicit nuclear reorganization. Indeed, stimulation of the MAP cascade by *GAL–STE11–Asp3* expression resulted in the same changes in nucleolar morphology as those seen after pheromone treatment (data not shown).

Finally, to test whether the *GAL–STE4*-induced changes in nuclear organization are mediated by downstream components of the pheromone-activated MAP kinase pathway, mutants in the pathway were coupled with *GAL–STE4* induction. The *STE12* gene encodes a transcription factor that is regulated by the MAP kinase pathway to activate genes required for the pheromone response. Significantly, reorganization of the nucleolus was not observed when *STE4* was induced in a *ste12* mutant (Figure 6d). The simplest explanation for this would be that the proteins responsible for nucleolar and nuclear reorganization are encoded by genes that are induced by Ste12p. To rule out the possibility that the lack of response in a *ste12* mutant reflects reduced transcription of upstream components of the MAP kinase pathway, which are themselves targets of Ste12p (see for example [40,41]), we checked whether *GAL–STE4* overexpression induces nucleolar reorganization in cells lacking the effector MAP kinases Fus3p and Kss1p, which activate the pheromone-response genes by phosphorylating the Ste12p ligands Dig1p and Dig2p. These inhibitors bind to and inhibit Ste12p, and appear to be released upon modification by MAP kinase [42,43]. In fact, the *fus3 kss1* double mutant fails to induce changes in nucleolar morphology, confirming that components critical for nucleolar reorganization are downstream of these kinases (Figure 6e).

To see if Ste12p itself regulates nuclear reorganization, we overexpressed an extrachromosomal copy of the gene *STE12*, which titrates out the inhibitory activity of Dig1p and Dig2p [44]. Importantly, induction of Ste12p not only leads to changes in nuclear structure in wild-type cells (data not shown), but also in cells defective for components of the MAP kinase pathway. We induced Ste12p in cells containing the *fus3-A* mutation (see Materials and methods, and [45]), and in cells disrupted for *ste11*, and monitored nuclear shape using GFP–Nup49. We found that ~40% of each population had dumbbell-shaped nuclei after Ste12p induction (Figure 7a–c). The absence of detectable shmoo tips in these same cells confirms that the MAP kinase Fus3p is non-functional [46,47]. A similar phenotype can be observed in the absence of *STE12* overexpression in a non-synchronized culture of cells deleted for *dig1*, *dig2* and *ste7* (Figure 7d). Here ~30% of the population showed dumbbell-shaped nuclei [42]. These results suggest that providing enough active Ste12p is sufficient to induce gross changes in nuclear shape in a significant fraction of the cells.

In summary, we have shown that induction of either *GAL–STE4* or *GAL–STE11* results in changes in nucleolar morphology, which in wild-type cells are dependent on the transcriptional activator Ste12p and the MAP kinases Fus3p and Kss1p. Nuclear shape changes also occur when Ste12p is activated, even if the MAP kinase cascade is blocked. Importantly, we see that a major restructuring of the nucleus and nucleolus, like transcriptional reprogramming, can occur in the absence of projection tip formation.

Figure 6

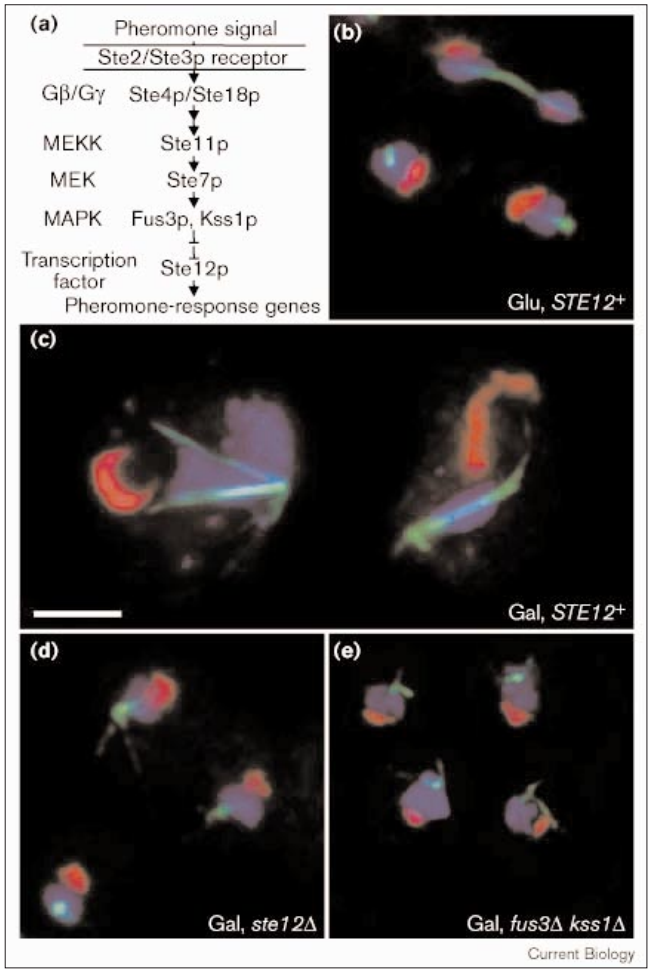

MAP kinase signaling through Ste12p induces nuclear reorganization. **(a)** The pheromone-response pathway of *S. cerevisiae.* For simplicity, only components relevant to the experiments described here are shown. **(b)** Cells in which the pheromone-response pathway was inhibited by growth in glucose medium. (**c–e)** Cells in which *STE4* was induced by galactose. Strains used are isogenic wild-type (*STE12*$^+$ (b,c)), *ste12::HIS3* (*ste12*Δ (d)) or *fus3::LEU2 kss1::HIS3* double mutant (*fus3*Δ*kss1*Δ (e)) transformed with a *GAL–STE4* plasmid. Cells were stained with anti-Nop1p antibodies to identify the nucleolus (red), anti-tubulin antibodies to identify microtubules (green) and DAPI to identify the chromosomal domain of the nucleus (blue). Results similar to those shown for *GAL–STE4* induction were obtained with MAP kinase activation by induction of *GAL–STE11–Asp3* (data not shown). Images were collected on a Leica DMRXA microscope. All images are of comparable scale, but *GAL–STE4*-induced cells, like pheromone-treated cells, become enlarged relative to untreated controls. The scale bar represents 2 μm.

Figure 7

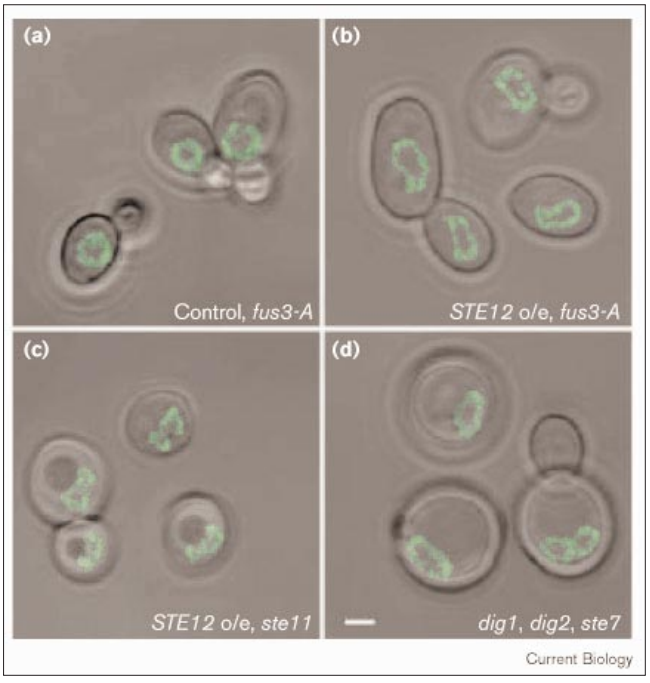

Changes in nuclear morphology are induced by overexpression of Ste12p in MAP kinase mutants. Expression of an extrachromosomal copy of Ste12p (*STE12* o/e) in **(a,b)** *fus3-A* (K2129) and **(c)** *ste11::ADE2* (YFD126) mutant strains in log phase has been inhibited by growth on glucose (control (a)) or induced for 2.5 h on galactose (*STE12* o/e (b,c)). Reorganization of nuclear morphology was visualized in living cells by direct fluorescence of the nuclear pore protein construct GFP–Nup49p. We used the catalytically inactive *fus3-A* mutant because it has a partial dominant-negative effect over Kss1p [57]. **(d)** Asynchronously growing *dig1*, *dig2*, *ste7* triple-mutant cells (MT1201) expressing GFP–Nup49p. In (b–d) activation of Ste12p results in a dumbbell-shaped nucleus in the absence of Fus3p, Ste11p or Ste7p activities. In the control sample (a) < 3% of nuclei are distorted. Images were collected in a Zeiss LSM 410 confocal microscope. The scale bar represents 2 μm.

Discussion

Pheromone signaling in yeast triggers a developmental switch that leads to altered programs of gene expression, gross rearrangement of cellular architecture, and ultimately to cell–cell fusion and diploidization. We have observed a striking reorganization of the nucleus in response to pheromone-induced signals, which yields two distinct nuclear domains and a reorganization of the nucleolar compartment. This rearrangement is independent of the microtubule- and actin-dependent changes in cellular morphology, but is fully dependent on the MAP kinase cascade and its downstream effectors, Fus3p/Kss1p and Ste12p.

In vegetatively growing cells, the nucleolus sits like a crescent-shaped cap within the nucleus, remaining in close contact with the rest of the genome. We note here that in pheromone-responding cells the nucleolus increases in volume and becomes spatially distinct from the rest of the genome, occupying one lobe of a dumbbell-shaped nucleus. This unique nuclear shape and change in nucleolar structure has not been described in previous studies of the pheromone response, which have focused primarily on localized cell growth and cytoskeletal changes [32,48]. This is due in part to the use of the DNA stain DAPI, which fails to label the nucleolus efficiently. Intriguingly, nucleolar function and pheromone signaling have been linked elsewhere through the yeast Ssf1 protein, which both localizes to the nucleolus and participates in projection tip formation [49].

Within the nucleolus of pheromone-responding cells, the transcriptional silencer Sir2p localizes to discrete subregions that colocalize with *in situ* hybridization signals for rDNA (E.M.S., unpublished observations). By examining this restricted subnucleolar Sir2p staining pattern, we monitor a unique extension of the rDNA fiber and an enlargement of the nucleolar domain in response to the MAP kinase cascade. The extended rDNA structure may facilitate pairing of chromosome XII homologs in preparation for meiosis, or it may simply reflect higher levels of rDNA transcription. Indeed, the rapid growth of pheromone-responding yeast cells is likely to require efficient protein synthesis and increased ribosome biosynthesis. Consistent with this, a recent microarray analysis has shown that *RRN10* and *RRN11*, the genes for two essential transcription factors for transcription by RNA polymerase I, are induced five- and eightfold, respectively, by Ste12p activation, although they are not equally induced by 2 h treatments with pheromone [50] (C. Boone, personal communication).

In addition to changes in nucleolar organization, we see that the nucleus assumes a distinct orientation with respect to the shmoo tip. The labeling of centromeres by FISH (E.M.S. and T.L., unpublished observations), as well as the labeling of telomeres (Figure 3b), reveals multiple signals in both cases, suggesting that neither centromeres nor telomeres coalesce into a single focus. All remain, however, within the lobe of the dumbbell-shaped nucleus that extends towards the spindle pole body and the projection tip. Unlike the elaborate horse-tail organization in the zygotic nucleus of fission yeast [8,9], the preconjugation nuclear reorganization reported here is not dependent on microtubule integrity, although correct orientation of the SPB towards the projection tip is. Thus, the rotational orientation of the nucleus, but not its compartmentation, may require kinesin activities that act in a polar fashion along cytoplasmic microtubules.

Nuclear organization is a target of the MAP kinase signaling cascade

Changes in both nuclear and nucleolar morphology are elicited by activation of the pheromone-response MAP kinase pathway. Not only can we block the reorganization

in mutants defective for MAP kinase signaling, but activation of the pathway in the absence of pheromone results in the same nuclear reorganization. We do not know whether *de novo* protein synthesis is required for the observed response. Activation of the transcriptional regulator Ste12p, however, seems to be a key event for eliciting changes in nuclear architecture. As Ste12p overexpression alone does not fully activate the MAP kinase cascade [46,47], and as activation of Ste12p in a *fus3* or *ste7* mutant brings about a significant level of nuclear reorganization, we suggest that Ste12p activation is not only necessary, but may be sufficient, to evoke at least some of the changes we observe. As the frequency of dumbbell-shaped nuclei is not as high in these mutants as in pheromone-treated cells, we cannot rule out an additional role for signals other than those arising from Ste12p activation. For example, structural nuclear proteins might be targets of the MAP kinase cascade, and might be necessary, together with the products of Ste12p-induced genes, for more subtle aspects of nucleolar or nuclear reorganization.

We have previously documented a pheromone-induced hyperphosphorylation of Sir3p and changes in transcriptional silencing of reporter genes at telomeres and the silent mating-type loci [33]. Despite this, we do not observe pheromone-induced changes in the localization of Rap1p, Sir3p or Sir4p, all of which are structural components of subtelomeric heterochromatin. Another MAP kinase target that is a structural component of chromatin is histone H3, modification of which correlates with both serum-induced gene induction and mitotic chromosome condensation in mammalian cells (reviewed in [51]). It will be important to examine the complete array of genes induced by Ste12p activation for components of the nucleolus or proteins that influence long-range chromatin order.

Conclusions

MAP kinase signaling induces changes in nuclear organization during the early stages of pheromone-induced conjugation in *S. cerevisiae*. Activation of the MAP kinase cascade itself results in similar changes, which are dependent on activation of the transcription factor Ste12p. Actin and microtubule polymerization are not necessary for the response. We propose that the signaling-induced restructuring has a role in the transcriptional reprogramming that accompanies conjugation, providing a new model to examine the relationship between patterns of gene expression and nuclear morphology.

Materials and methods

Yeast strains, plasmids and growth conditions

The *MAT***a**/*MAT***a** diploid LPY2686 was made from the haploid strain 1255-5C (*MAT***a** *ade1 bar2 his2 leu2 trp1 ura3* [33]) by mating-type switching in two steps with the use of a plasmid carrying the *HO* gene. Other strains used are LPY1683 (*MAT***a** *ade2-101 his3-Δ200 leu2-Δ1 lys2-801 trp1-Δ63 ura3-52 adh4::URA3-TELVIIL DIA5-1ADE2-TELVR*) [33], LPY3252 (= LPY1683 *ste12::HIS3*), EY957 (W303-1a *bar1* = *MAT***a** *ade2-1 his3-11,15 leu2-3,112 trp1-1 ura3-1 can1-100 bar1*), EY966 (= EY957 *fus3::LEU2 kss1::HIS3*; kindly provided by E. Elion, Harvard Medical School), K2129 (W303-1a *bar1::HISG fus3-A*; kindly provided by G. Ammerer, IMP, Vienna) and YFD 126 (W303-1a *bar1-1 ste11::ADE2*; kindly provided by M. Peter, ISREC). LPY3252 was disrupted for *STE12* by PCR-directed deletion of the open reading frame [52]. Plasmids introduced include p*GAL–STE4*, p*GAL–STE4*-Asp3 and p*GAL–STE12* [52], which are repressed or induced after growth in 2% raffinose-containing medium by adding glucose or galactose to 2% for 4–6 h. Growth conditions for G1 cyclin depletion using haploid strain 1608-21C (= 1255-5C *cln1 cln2 cln3 leu2::LEU2::GAL-CLN3*) or GA-1163 (see below) are described in the Supplementary material. The GFP–NUP49 fusion gene [53] (kindly provided by V. Doye, CNRS, Institut Curie) was inserted into various yeast vectors for expression or integration. Integration into LPY2686 created strain GA-1109, and into 1608-21C created strain GA-1163. The same construct was introduced into K2129 and YFD126, containing p*GAL–STE12* and MT1201 (*dig1::URA3 dig2::HIS3 ste7::LEU2*; kindly provided by M. Tyers, University of Toronto). GA-1096 (*MAT***a**, *ade2 leu2, his3, ura3, trp1, nup49::TRP1*, with the plasmid pUN100–GFP–NUP49) was used for the mating assay in Figure 1.

Antisera, indirect immunofluorescence and FISH

Preparation, characterization and affinity purification of polyclonal rabbit antisera were previously described [6,21]. Antibodies against actin (mouse monoclonal C4; Boehringer Mannheim), tubulin (mouse monoclonal TAT-1 [54]) and secondary antibodies are described elsewhere [6]. Cells were prepared for immunofluorescence and FISH by adjusting the culture to 3.3% formaldehyde for 10 min at 30°C. Fixed cells were then washed twice in YPD, and spheroplasted as described [55] except that three times more enzyme was added. FISH and immunostaining were performed as described in [55]. Microscopy techniques are available on the web.

Supplementary material

Additional methodological details are available at http://current-biology.com/supmat/supmatin.htm.

Acknowledgements

We thank M. Gotta, I. Hagan, M. Peter, H. Renauld, F. van Drogen, M. Blondel, M. Winey and members of the Pillus laboratory for many helpful discussions; M. Gotta, M. Peter, J. Rine, F. Solomon, J. Aris, E. Hurt, V. Doye, M. Tyers, G. Ammerer, and E. Elion for reagents; O. Dreesen for technical assistance; and B. Betz, J. R. McIntosh, and K. Pogliano for use of fluorescence microscope facilities. Microscopy was made possible in part by a gift from Virginia and Mel Clark. We thank H. Browning, C. Chapon, S. Jacobson, F. Luca, M. Peter, E. Weiss, and R. West for critically reading the manuscript. E.M.S. gratefully acknowledges the Huggenberger-Bischoff Foundation for sponsoring a research visit to Switzerland. P.H. thanks Boehringer-Ingelheim Fonds for a doctoral fellowship. Research in the Pillus laboratory is funded by the National Institutes of Health. The Gasser laboratory is grateful for support from the Human Frontiers Science Program, the Swiss National Science Foundation, and the Swiss League against Cancer.

References

1. Lamond AI, Earnshaw WC: **Structure and function in the nucleus**. *Science* 1998, **280:**547-553.
2. Misteli T, Caceres JF, Spector DL: **The dynamics of a pre-mRNA splicing factor in living cells**. *Nature* 1997, **387:**523-527.
3. Coverley D, Laskey RA: **Regulation of eukaryotic DNA replication**. *Annu Rev Biochem* 1994, **63:**745-776.
4. Cremer T, Kurz A, Zirbel R, Dietzel S, Rinke B, Schrock E, *et al.*: **Role of chromosome territories in the functional compartmentalization of the cell nucleus**. *Cold Spring Harbor Symp Quant Biol* 1993, **58:**777-792.
5. Hochstrasser M, Mathog D, Gruenbaum Y, Saumweber H, Sedat JW: **Spatial organization of chromosomes in the salivary gland nuclei of *Drosophila melanogaster***. *J Cell Biol* 1986, **102:**112-123.
6. Gotta M, Laroche T, Formenton A, Maillet L, Scherthan H, Gasser SM: **The clustering of telomeres and colocalization with Rap1, Sir3, and Sir4 proteins in wild-type *Saccharomyces cerevisiae***. *J Cell Biol* 1996, **134:**1349-1363.

7. Laroche T, Martin SG, Tsai-Pflugfelder M, Gasser SM: **The dynamics of yeast telomeres and silencing proteins through the cell cycle**. *J Struct Biol* 2000, in press.
8. Chikashige Y, Ding DQ, Funabiki H, Haraguchi T, Mashiko S, Yanagida M*, et al.*: **Telomere-led premeiotic chromosome movement in fission yeast**. *Science* 1994, **264:**270-273.
9. Chikashige Y, Ding DQ, Imai Y, Yamamoto M, Haraguchi T, Hiraoka Y: **Meiotic nuclear reorganization: switching the position of centromeres and telomeres in the fission yeast *Schizosaccharomyces pombe***. *EMBO J* 1997, **16:**193-202.
10. Cooper JP, Watanabe Y, Nurse P: **Fission yeast Taz1 protein is required for meiotic telomere clustering and recombination**. *Nature* 1998, **392:**828-831.
11. Nimmo ER, Pidoux AL, Perry PE, Allshire RC: **Defective meiosis in telomere-silencing mutants of *Schizosaccharomyces pombe***. *Nature* 1998, **392**:825-828.
12. Boulton SJ, Jackson SP: **Components of the Ku-dependent non-homologous end-joining pathway are involved in telomeric length maintenance and telomeric silencing**. *EMBO J* 1998, **17:**1819-1828.
13. Laroche T, Martin SG, Gotta M, Gorham HC, Pryde FE, Louis EJ*, et al.*: **Mutation of yeast Ku genes disrupts the subnuclear organization of telomeres**. *Curr Biol* 1998, **8:**653-656.
14. Pryde FE, Gorham HC, Louis EJ: **Chromosome ends: all the same under their caps**. *Curr Opin Genet Dev* 1997, **7:**822-828.
15. Klein F, Laroche T, Cardenas ME, Hofmann JF, Schweizer D, Gasser SM: **Localization of RAP1 and topoisomerase II in nuclei and meiotic chromosomes of yeast**. *J Cell Biol* 1992, **117:**935-948.
16. Guacci V, Hogan E, Koshland D: **Centromere position in budding yeast: evidence for anaphase A**. *Mol Biol Cell* 1997, **8:**957-972.
17. Straight AF, Marshall WF, Sedat JW, Murray AW: **Mitosis in living budding yeast: anaphase A but no metaphase plate**. *Science* 1997, **277:**574-578.
18. Jin Q, Trelles-Sticken E, Scherthan H, Loidl J: **Yeast nuclei display prominent centromere clustering that is reduced in nondividing cells and in meiotic prophase**. *J Cell Biol* 1998, **141:**21-29.
19. Hayashi A, Ogawa H, Kohno K, Gasser SM, Hiraoka Y: **Meiotic behaviours of chromosomes and microtubules in budding yeast: relocalization of centromeres and telomeres during meiotic prophase**. *Genes Cells* 1998, **3:**587-601.
20. Trelles-Sticken E, Loidl J, Scherthan H: **Bouquet formation in budding yeast: initiation of recombination is not required for meiotic telomere clustering**. *J Cell Sci* 1999, **112:**651-658.
21. Gotta M, Strahl-Bolsinger S, Renauld H, Laroche T, Kennedy BK, Grunstein M*, et al.*: **Localization of Sir2p: the nucleolus as a compartment for silent information regulators**. *EMBO J* 1997, **16:**3243-3255.
22. Suja JA, Gebrane-Younes J, Geraud G, Hernandez-Verdun D: **Relative distribution of rDNA and proteins of the RNA polymerase I transcription machinery at chromosomal NORs**. *Chromosoma* 1997, **105:**459-469.
23. Nierras CR, Liebman SW, Warner JR: **Does *Saccharomyces* need an organized nucleolus?** *Chromosoma* 1997, **105:**444-451.
24. Oakes M, Aris JP, Brockenbrough JS, Wai H, Vu L, Nomura M: **Mutational analysis of the structure and localization of the nucleolus in the yeast *Saccharomyces cerevisiae***. *J Cell Biol* 1998, **143:**23-34.
25. Sinclair DA, Mills K, Guarente L: **Accelerated aging and nucleolar fragmentation in yeast sgs1 mutants**. *Science* 1997, **277:**1313-1316.
26. Herskowitz I: **MAP kinase pathways in yeast: for mating and more**. *Cell* 1995, **80:**187-197.
27. Rose MD: **Nuclear fusion in the yeast *Saccharomyces cerevisiae***. *Annu Rev Cell Dev Biol* 1996, **12:**663-695.
28. Byers B, Goetsch L: **Duplication of spindle plaques and integration of the yeast cell cycle**. *Cold Spring Harbor Symp Quant Biol* 1974, **38:**123-131.
29. Baba N, Baba M, Imamura M, Koga M, Ohsumi Y, Osumi M*, et al.*: **Serial section reconstruction using a computer graphics system: applications to intracellular structures in yeast cells and to the periodontal structure of dogs' teeth**. *J Electron Microsc Techn* 1989, **11:**16-26.
30. Meluh PB, Rose MD: **KAR3, a kinesin-related gene required for yeast nuclear fusion**. *Cell* 1990, **60:**1029-1041.
31. Maddox P, Chin E, Mallavarapu A, Yeh E, Salmon ED: **Microtubule dynamics from mating through the first zygotic division in the budding yeast *Saccharomyces cerevisiae***. *J Cell Biol* 1999, **144:**977-987.
32. Read EB, Okamura HH, Drubin DG: **Actin- and tubulin-dependent functions during *Saccharomyces cerevisiae* mating projection formation**. *Mol Biol Cell* 1992, **3:**429-444.
33. Stone EM, Pillus L: **Activation of an MAP kinase cascade leads to Sir3p hyperphosphorylation and strengthens transcriptional silencing**. *J Cell Biol* 1996, **135:**571-583.
34. Aparicio OM, Billington BL, Gottschling DE: **Modifiers of position effect are shared between telomeric and silent mating-type loci in *S. cerevisiae***. *Cell* 1991, **66:**1279-1287.
35. Bryk M, Banerjee M, Murphy M, Knudsen KE, Garfinkel DJ, Curcio MJ: **Transcriptional silencing of Ty1 elements in the RDN1 locus of yeast**. *Genes Dev* 1997, **11:**255-269.
36. Smith JS, Boeke JD: **An unusual form of transcriptional silencing in yeast ribosomal DNA**. *Genes Dev* 1997, **11:**241-254.
37. Fritze CE, Verschueren K, Strich R, Easton Esposito R: **Direct evidence for SIR2 modulation of chromatin structure in yeast rDNA**. *EMBO J* 1997, **16:**6495-6509.
38. Yang CH, Lambie EJ, Hardin J, Craft J, Snyder M: **Higher order structure is present in the yeast nucleus: autoantibody probes demonstrate that the nucleolus lies opposite the spindle pole body**. *Chromosoma* 1989, **98:**123-128.
39. Ayscough KR, Drubin DG: **A role for the yeast actin cytoskeleton in pheromone receptor clustering and signalling**. *Curr Biol* 1998, **8:**927-930.
40. Fields S, Chaleff DT, Sprague GF Jr: **Yeast STE7, STE11, and STE12 genes are required for expression of cell-type-specific genes**. *Mol Cell Biol* 1988, **8:**551-556.
41. Elion EA, Brill JA, Fink GR: **Functional redundancy in the yeast cell cycle: FUS3 and KSS1 have both overlapping and unique functions**. *Cold Spring Harbor Symp Quant Biol* 1991, **56:**41-49.
42. Tedford K, Kim S, Sa D, Stevens K, Tyers M: **Regulation of the mating pheromone and invasive growth responses in yeast by two MAP kinase substrates**. *Curr Biol* 1997, **7:**228-238.
43. Bardwell L, Cook JG, Zhu-Shimoni JX, Voora D, Thorner J: **Differential regulation of transcription: repression by unactivated mitogen-activated protein kinase Kss1 requires the Dig1 and Dig2 proteins**. *Proc Natl Acad Sci USA* 1998, **95:**15400-15405.
44. Dolan JW, Fields S: **Overproduction of the yeast STE12 protein leads to constitutive transcriptional induction**. *Genes Dev* 1990, **4**:492-502.
45. Gartner A, Jovanovic A, Jeoung DI, Bourlat S, Cross FR, Ammerer G: **Pheromone-dependent G1 cell cycle arrest requires Far1 phosphorylation, but may not involve inhibition of Cdc28-Cln2 kinase, *in vivo***. *Mol Cell Biol* 1998, **18:**3681-3691.
46. Peter M, Gartner A, Horecka J, Ammerer G, Herskowitz I: **FAR1 links the signal transduction pathway to the cell cycle machinery in yeast**. *Cell* 1993, **73:**747-760.
47. Farley FW, Satterberg B, Goldsmith EJ, Elion EA: **Relative dependence of different outputs of the *Saccharomyces cerevisiae* pheromone response pathway on the MAP kinase Fus3p**. *Genetics* 1999, **151:**1425-1444.
48. Trueheart J, Boeke JD, Fink GR: **Two genes required for cell fusion during yeast conjugation: evidence for a pheromone-induced surface protein**. *Mol Cell Biol* 1987, **7:**2316-2328.
49. Kim J, Hirsch JP: **A nucleolar protein that affects mating efficiency in *Saccharomyces cerevisiae* by altering the morphological response to pheromone**. *Genetics* 1998, **149:**795-805.
50. Roberts CJ, Nelson B, Marton MJ, Stoughton R, Meyer MR, *et al.*: **Signaling and circuitry of multiple MAPK pathways revealed by a matrix of global gene expression profiles.** *Science* 2000, **287:**873-880.
51. Strahl BD, Allis CD: **The language of covalent histone modifications**. *Nature* 2000, **403:**41-45.
52. Adams A, Gottschling DE, Kaiser CA, Stearns T: *Methods in Yeast Genetics*. New York: Cold Spring Harbor Laboratory Press; 1997.
53. Belgareh N, Doye V: **Dynamics of nuclear pore distribution in nucleoporin mutant yeast cells**. *J Cell Biol* 1997, **136:**747-759.
54. Woods A, Sherwin T, Sasse R, MacRae TH, Baines AJ, Gull K: **Definition of individual components within the cytoskeleton of *Trypanosoma brucei* by a library of monoclonal antibodies**. *J Cell Sci* 1989, **93:**491-500.
55. Gotta M, Laroche T, Gasser SM: **Analysis of nuclear organization in *Saccharomyces cerevisiae***. *Methods Enzymol* 1999, **304:**663-672.
56. McKinney JD, Chang F, Heintz N, Cross FR: **Negative regulation of FAR1 at the start of the yeast cell cycle**. *Genes Dev* 1993, **7:**833-843.
57. Madhani HD, Styles CA, Fink GR: **MAP kinases with distinct inhibitory functions impart signaling specificity during yeast differentiation**. *Cell* 1997, **91:**673-684.